In-Situ Microscopy Observations of Oxide Phases Formation During High-Temperature Oxidation of End-of-Life Ni/Cu/Ni-Coated-NdFeB Permanent Magnets

D. C. Nababan, R. Mukhlis, Y. Durandet, M. I. Pownceby, L. Prentice, and M. A. Rhamdhani

Abstract An understanding of the reaction phases formed during the high-temperature oxidation of rare earth permanent magnets is vital for developing appropriate strategies for their pyrometallurgy-based recycling processes aimed at the concentration and potential recovery of the rare earth elements. The current study uses in-situ high-temperature optical microscopy combined with ex-situ scanning electron microscopy to analyze oxide growth on the surface of an end-of-life Ni/Cu/Ni-coated NdFeB permanent magnet oxidized at 900 and 1100 °C for up to 4 h under ambient air conditions. Distinct oxide morphologies were observed at the two oxidation temperatures over time ranging from blister- and spike-like structures. At the longest oxidation times, visible cracking of the surface of the magnet and protrusion of Fe_2O_3 phase were observed. The presence of a Ni/Cu/Ni coating on the magnets was found to significantly affect the oxidation growth; a nickel ferrite phase was formed at 1100 °C after 4 h while at 900 °C, there was still discrete NiO and Fe_2O_3.

Keywords Rare earth · NdFeB magnet · High-temperature oxidation · Hot-stage microscopy

D. C. Nababan (✉) · R. Mukhlis · Y. Durandet · M. A. Rhamdhani
Fluid and Process Dynamics (FPD) Group, Department Mechanical and Product Design Engineering, Swinburne University of Technology, Melbourne, VIC 3122, Australia
e-mail: dnababan@swin.edu.au

M. A. Rhamdhani
e-mail: arhamdhani@swin.edu.au

M. I. Pownceby
CSIRO Mineral Resources, Clayton, Melbourne, VIC 3169, Australia

L. Prentice
CSIRO Manufacturing, Clayton, Melbourne, VIC 3169, Australia

Introduction

Neodymium-iron-boron (NdFeB) rare earth permanent magnets (REPM) have a wide range of applications including in electric vehicles [1], wind power turbines [2], and computer hard disk drives [3]. Typical NdFeB magnets contain up to 32 wt% of rare earth elements (REEs) which is dominated by the light REE, neodymium (Nd) [4]), but with minor praseodymium (Pr) and dysprosium (Dy) also present. Recycling of end-of-life (EOL) NdFeB permanent magnets will be vital to support the expected growth in global demand for Nd and Dy, due to the fact that these metals had significant supply shortfalls in the recent past. In addition, direct mining of REEs from ores generates many issues with regard to the environment as their minerals commonly contain trace to minor radioactive elements such as uranium and thorium [5].

The recycling of NdFeB magnets can be carried out through pyrometallurgy, hydrometallurgy, and their combined routes [6–8]. Despite the challenges associated with its high-temperature requirement, the pyrometallurgy route offers some advantages especially when renewable energy sources such as concentrated solar energy are applied to supply the heat. In the pyrometallurgy approach, the oxidation behavior of the EOL NdFeB magnet at high temperatures will govern how the materials will be processed in the subsequent steps, as well as its overall recycling process. The aim of this oxidation step is to transform the REEs form into REE-oxides where further processing would more easily take place.

In the context of recycling, there have been several studies regarding the high-temperature oxidation of NdFeB magnets available in the literature. Firdaus et al. [9–12] conducted oxidation studies in the range of 700–1200 °C. using new uncoated magnets as the starting samples, observed the formation of Fe_2O_3 on the outer oxide layer while the Nd was concentrated mainly in the form of $NdFeO_3$ underneath, particularly during the oxidation at the range of 1000–1200 °C. Using the same temperature range, a similar pattern was also observed by Nababan et al. [5, 13] which used Ni/Cu/Ni-coated EOL NdFeB magnets. This suggested that the Fe was diffused outward while the Ni and Cu diffused inward and reacted with the formed Fe_2O_3. The formation of Fe_2O_3 on the surface was a significant finding which has an important implication on the general mechanism of concentrating both Fe and REEs.

More detailed mechanistic studies of the oxide growth on the surface of NdFeB magnets are still limited. This current study is focused on directly observing the growth of oxide(s) on the surface of Ni/Cu/Ni-coated EOL NdFeB magnets in the early stage of oxidation at 900 and 1100 °C. In-situ high-temperature optical microscopy combined with *ex-situ* scanning electron microscopy was used to analyze the oxide growth on the surface for an oxidation period of four hours under ambient air conditions.

Table 1 Chemical composition of typical REPM samples (wt%)

Item	Element									
	Nd	Pr	Dy	Fe	B	Nb	Co	Al	Ni	Cu
EOL NdFeB magnet used in this work	17.0	5.4	4.51	68.43	1.0	0.16	0.93	1.0	0.85	0.72

Methodology

Sample Preparation

The EOL NdFeB magnet samples used in this study were obtained from Note Printing Australia Ltd., Australia, and were previously used in banknote machine printing. Inductively Coupled Plasma Optical Emission Spectrometry (ICP-OES) was used to determine the chemical composition of the magnets, and the results are shown in Table 1.

The samples were firstly cleaned in an ultrasonic cleaner in acetone medium to ensure any contaminants were removed from the surface. This was followed by thermally demagnetization of the samples at 300 °C for 30 min in an oven. This step was not found to oxidize the samples or change their microstructure.

Sample Characterization

The microstructure observation and surface analysis of the original magnet and the oxidized EOL NdFeB magnet samples were carried out using Scanning Electron Microscope (SEM) equipped with Energy Dispersive X-ray (EDX) spectroscopy (for generating elemental distribution maps and providing semi-quantitative chemical composition analyses). Figure 1 shows the cross-sectional microstructure of the original NdFeB magnet used in this study. It shows the Ni/Cu/Ni coating layer on the surface of the magnet with a thickness of approximately 20 μm as well as the two main matrix phases in the magnet, i.e. the Φ phase ($Nd_2Fe_{14}B$) as the main matrix phase and an Nd-rich phase typically at grain boundaries.

Experimental Techniques

The oxidation experiment was conducted using Linkam Scientific hot-stage coupled with an optical microscope (Olympus). The experiments were conducted at 900 and 1100 °C with the longest duration heating experiment being four hours. The setup can be seen in Fig. 2. The sample was placed under a lens in the hot stage surrounded by heating elements. Two flanges were kept open to allow the ambient air to circulate.
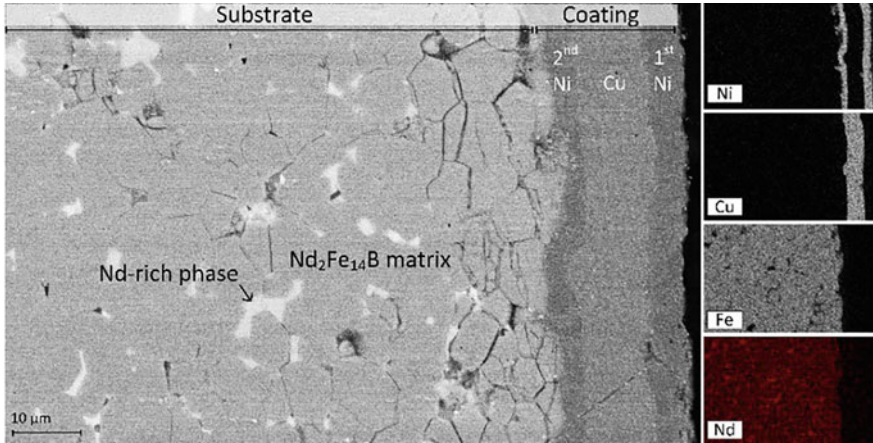
Fig. 1 SEM back-scattered image showing the typical microstructure of the EOL NdFeB magnet used in this study. The image shows the Ni/Cu/Ni coating layer, the intergranular Nd-rich phase, and the main Φ matrix phase ($Nd_2Fe_{14}B$). Also included are corresponding EDX elemental maps showing the distribution of the elements Fe, Cu, Ni, and Nd

A lid with a water-cooling system was installed to protect the direct exposure of the heat on the lens. The heating rate on each experiment was set to 150 °C/min.
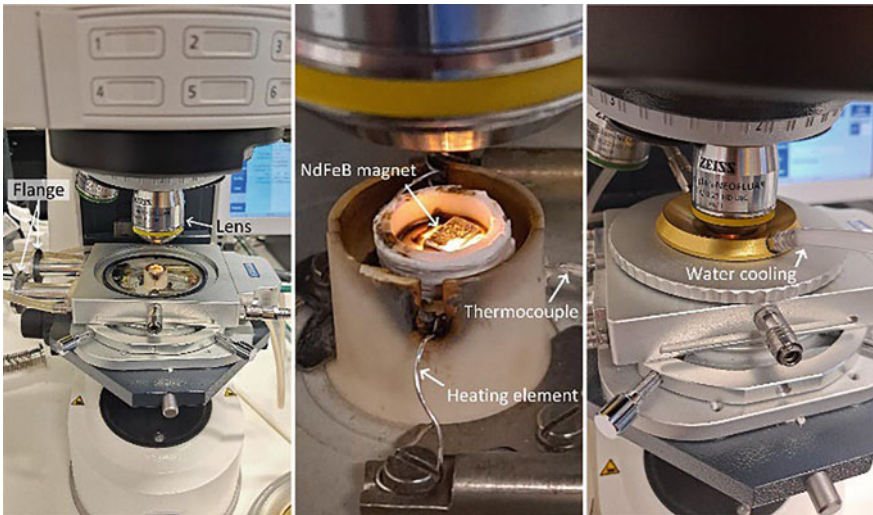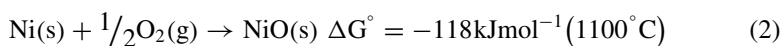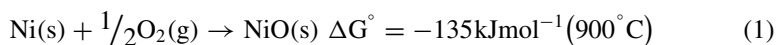

Fig. 2 Hot-stage microscopy apparatus used in this study

Results and Discussion

Previous works by the authors [5, 13] studied the high-temperature oxidation of the EOL NdFeB magnet through microstructural observations of cross-sections of oxidized-samples. This current work aims to carry out a complementary, but more detailed observation of magnet's oxidation behavior by focusing on the oxide growth on the surface in the early stages. Two oxidation temperatures, 900 and 1100 °C, were selected in the current study.

Oxide Growth Observation During the High-Temperature Oxidation of NdFeB Permanent Magnets at 900 °C

Figure 3 shows the optical images obtained from oxidation of a NdFeB magnet at 900 °C. The heating time to reach the target temperature was approximately six minutes. It is important to note that the untreated surface of the magnet had some surface imperfections (valleys) formed during its manufacturing process. Once the temperature reached 900 °C, the surface was already fully covered by NiO which formed due to the oxidation of the 1st Ni layer on the coating surface according to Reactions (1) and (2) below:

$$Ni(s) + ^1/_2O_2(g) \rightarrow NiO(s) \ \Delta G^\circ = -135 kJmol^{-1}(900^\circ C) \tag{1}$$

$$Ni(s) + ^1/_2O_2(g) \rightarrow NiO(s) \ \Delta G^\circ = -118 kJmol^{-1}(1100^\circ C) \tag{2}$$

As the oxidation proceeded, after about 13 min, another oxide (predicted to be Fe_2O_3) was observed to begin growing on the surface. The former nickel oxide continued to grow bigger while some Fe_2O_3 was formed at other locations. A crack on the NiO surface was observed after 50 min while at the same time, a distending surface was observed. The crack continued to form and grow larger, particularly on the distending surface. As clearly indicated in Fig. 3 at 170 and 240 min, the NiO surface was cracked and significantly distended caused by the growth of Fe_2O_3 underneath.

The ex-situ SEM examination of the surface of the oxidized NdFeB magnet after 240 min of heating at 900 °C is shown in Fig. 4a. Also shown are results from with the EDX mapping from a smaller region in Fig. 4d. Results show the surface was covered by a NiO layer with some cracks present. Figure 4c shows spiky Fe_2O_3 growing out from underneath the NiO, thereby generating further cracks on the surface. The growth of spiky Fe_2O_3 phase is shown in Fig. 4e where the Fe_2O_3 continued to grow outward and to the side. Figure 4b, d shows the Fe_2O_3 that has grown along, and penetrated through, the surface cracks.
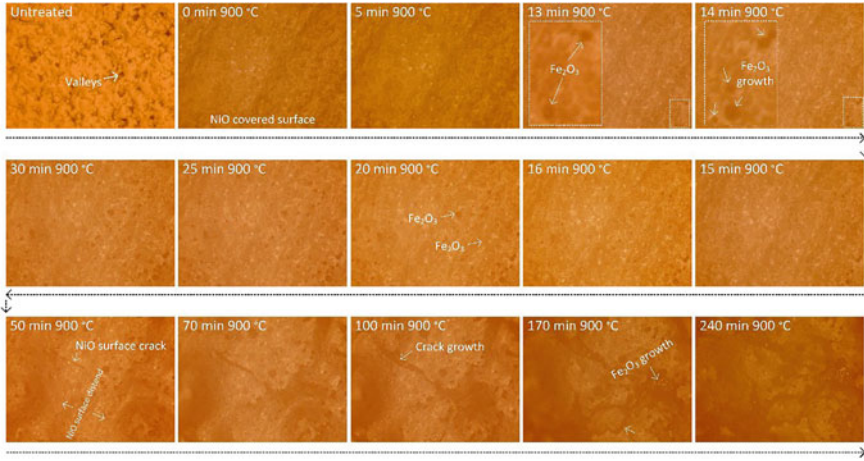
Fig. 3 Hot-stage microscope images of EOL NdFeB magnet's surface oxidized at 900 °C for 4 h in air. The heating rate is 150 °C/min
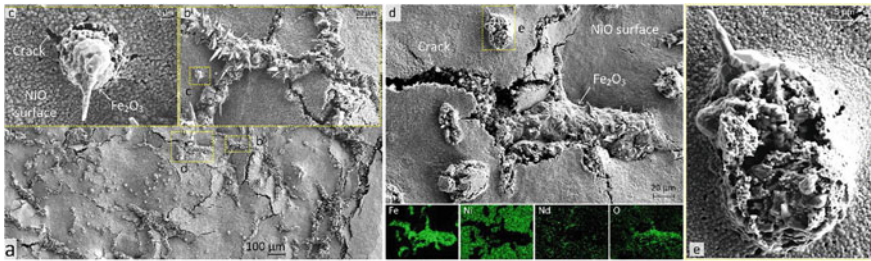

Fig. 4 SEM secondary electron images showing the surface of EOL NdFeB magnet sample oxidized at 900 °C for 4 h in air. Also included are EDX element distribution map results showing the distribution of O, Fe, Ni, and Nd across a selected imaged area (shown in Fig. 4d)

Oxide Growth Observation During the High-Temperature Oxidation of NdFeB Permanent Magnets at 1100 °C

Figure 5 shows the transformation over time of the surface morphology of the NdFeB magnet during the oxidation heating process up to 1100 °C under air atmosphere. The hot-stage microscopy images were taken in one heating sequence with one sample. The SEM images, however, were taken separately following a discontinued heating process, i.e. one representative image was taken from each sample after heating to a particular temperature.

Similar to the observations at 900 °C, the untreated surface of the magnet had some surface imperfections (valleys) formed during its manufacturing process. At the early oxidation stages, up to 500 °C, reflections with distinct colors were captured which
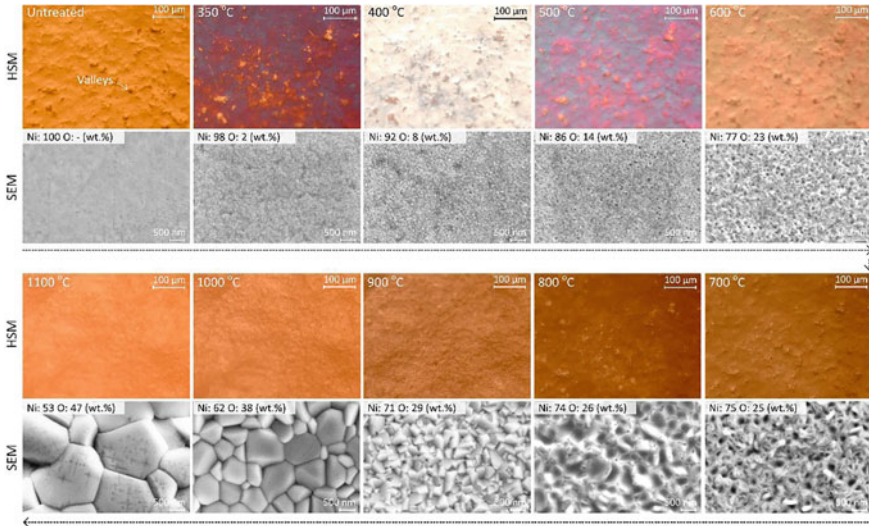
Fig. 5 Hot-stage microscopy coupled with SEM images of EOL NdFeB magnet's surface heated-oxidized at 350–1100 °C in air. The heating rate was 150 °C/min

might indicate changes in the surface's morphology and/or chemical composition. The SEM images indicated significant grain growth (fine-grained) on the surface, and the EDX analysis confirmed an increase of oxygen concentration. It is plausible to suggest that the NiO was already formed during the heating stage. At temperatures higher than 600 °C, the surface reflections showed a relatively homogeneous color which might indicate that the whole surface was fully covered by the NiO. As the heating and oxidation continued to proceed, the oxygen concentration was increased up to 47 wt.% at 1100 °C where NiO grain growth was pronounced.

Figure 6 shows the microscopy images during the oxidation of NdFeB magnets at 1100 °C for 4 h, a continuation of the experiment presented in Fig. 5. It can be seen that another oxide (indicated by arrows) grew immediately after 1 min oxidation. The previous study [5] observed that the NiO layer on the surface was dissolved and reacted with Fe_2O_3 as the oxidation proceeded which grew outward to form the spinel phase $NiFe_2O_4$. For simplification, this study assumed that the formed oxide was $NiFe_2O_4$ whereas the EDX result presented in Table 2 shows the approximate composition of the oxide as, 36 wt.% O, 52 wt.% Fe, and 11 wt.% Ni. The reaction might follow the Reaction (3):

$$NiO(s) + Fe_2O_3(s) \rightarrow NiFe_2O_4(s) \tag{3}$$
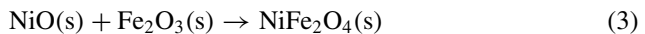
The nucleation of $NiFe_2O_4$ occurred in several different locations after a certain period of time (e.g. 5 min), and the $NiFe_2O_4$ continued to grow and merge with the
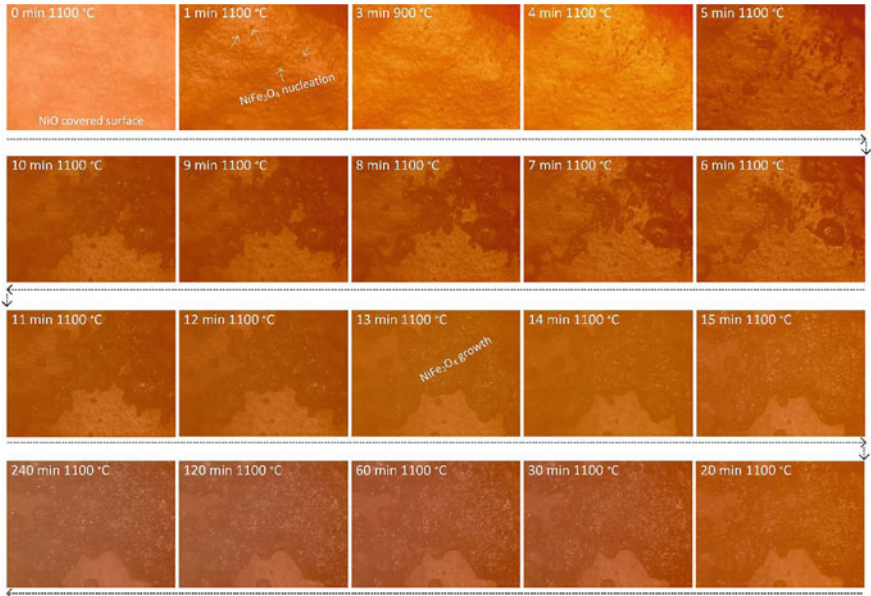
Fig. 6 Hot-stage microscope images of EOL NdFeB magnet's surface oxidized at 1100 °C for 4 h

Table 2 EDX semi-quantitative composition analysis including the deduced phase from points 1–4 in Fig. 7

Element (wt%)	Point			
	1	2	3	4
O	28.88	36.09	30.92	30.06
Fe	12.62	52.72	10.69	21.74
Ni	58.50	11.19	58.39	48.20
Deduced main phase	NiO	$NiFe_2O_4$	NiO	–

Table 3 EDX semi-quantitative composition analysis including the deduced phase from points 1–10 in Fig. 9

Element (wt%)	Point			
	1	2	3	4
O	27.42	32.16	27.70	30.25
Fe	5.23	66.80	27.70	4.96
Ni	67.35	1.04	5.12	64.79
Deduced main phase	NiO	$NiFe_2O_4$	Fe_2O_3	NiO

other surrounding $NiFe_2O_4$. The $NiFe_2O_4$ layer almost fully covered the surface of the magnet after 60 min of reaction time.

Figure 7 shows SEM images of the surface of a NdFeB magnet oxidized at 1100 °C for 1 min, using SE and back-scattered (BSE) modes and with semi-quantitative EDX point analysis. The locations of the EDX point analyses are also given in Fig. 7, and the results are presented in Table 2. Figure 7b–e illustrates the early stage of $NiFe_2O_4$ formation. In Fig. 7d, Point 1 shows that the surface is dominated by Ni, 58.5 wt% with the Fe being 11.19 wt.% whereas Point 3 has a similar composition. For simplicity, this phase was called NiO (with Fe in solution). It is interesting to see another phase, with black color, formed on the NiO phase, marked by Point 4 with a higher amount of Fe, 21.74 wt.%. This might indicate the outward diffusion of Fe to react with NiO. As the Fe continued to diffuse outwardly and react with NiO, the $NiFe_2O_4$ formed bigger sized crystals and distended in shape (particle labelled as 2 in Fig. 7d). EDX analysis confirmed an increasing amount of Fe up to 52.72 wt.% was associated with this phase. Furthermore, Fig. 7e shows that some blisters coalesced with their surroundings. Figure 8 shows the surface of an oxidized NdFeB magnet at 1100 °C for 5 min where it shows that the $NiFe_2O_4$ blisters were formed at different spots and with the former blisters continuing to grow over time as shown in Fig. 8b.

The microscopy images provided in Fig. 6 show that after being oxidized for 4 h, the formed oxides, which are dominated by $NiFe_2O_4$, had partially covered the surface. Figures 9a, b show the SE/BSE SEM observation of the sample's surface. Figure 9a shows a layer of spiky oxide covering some area on the surface of the magnet with Fig. 9c showing a bigger magnification of a specific area in Fig. 9a. Based on the EDX result, the outer oxide layer was dominated by Fe, marked by Point 2, with a composition of Fe up to 66.80 wt% whereas the surface area covered
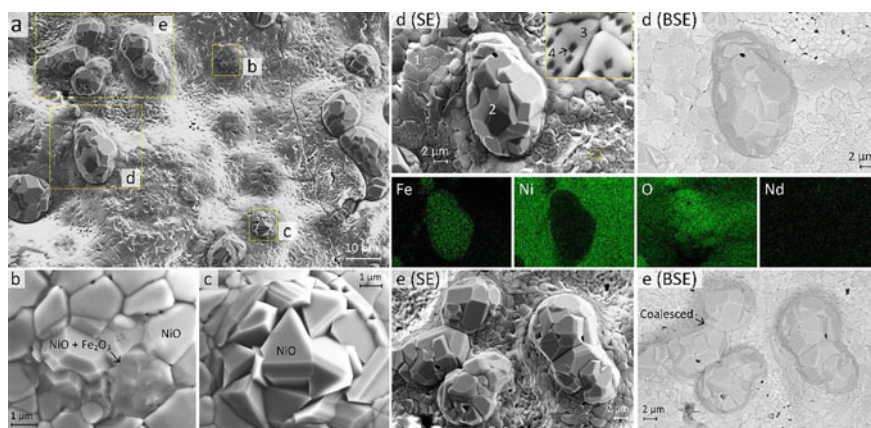

Fig. 7 SEM secondary electron and back-scattered electron images showing the surface of EOL NdFeB magnet sample oxidized at 1100 °C for 1 min. Also included are EDX element distribution maps for O, Fe, Ni, and Nd across the selected imaged area
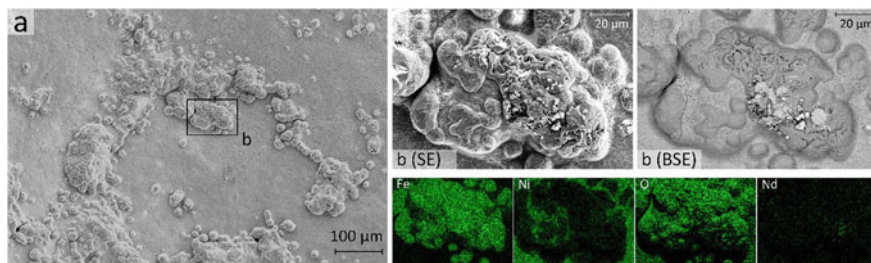
Fig. 8 SEM secondary electron and back-scattered electron images showing the surface of EOL NdFeB magnet sample oxidized at 1100 °C for 5 min. Also included are EDX element distribution maps for O, Fe, Ni, and Nd across the selected imaged area

by NiO was still present, marked by number 1, with a composition of Ni up to 67.35 wt%. The other area provided in Fig. 9b shows a similar observation to the oxidation at 900 °C. Instead of reacting with the NiO, the Fe_2O_3 cleaved the NiO to grow with a spiky shape. This might occur due to the spalling of NiO which allowed the Fe_2O_3 to grow outward directly instead of reacting with the NiO.

The previous works [5, 13] showed that at higher temperatures (900–1200 °C), the Cu and Ni (from the 2nd Ni layer), as the components of the coating, diffused inward through the Nd-rich matrix phase in the substrate where the 1st Ni layer on the surface was oxidized immediately to NiO. With longer oxidation time at 900 °C, the thin dense layer of NiO still remained on the surface. The observation
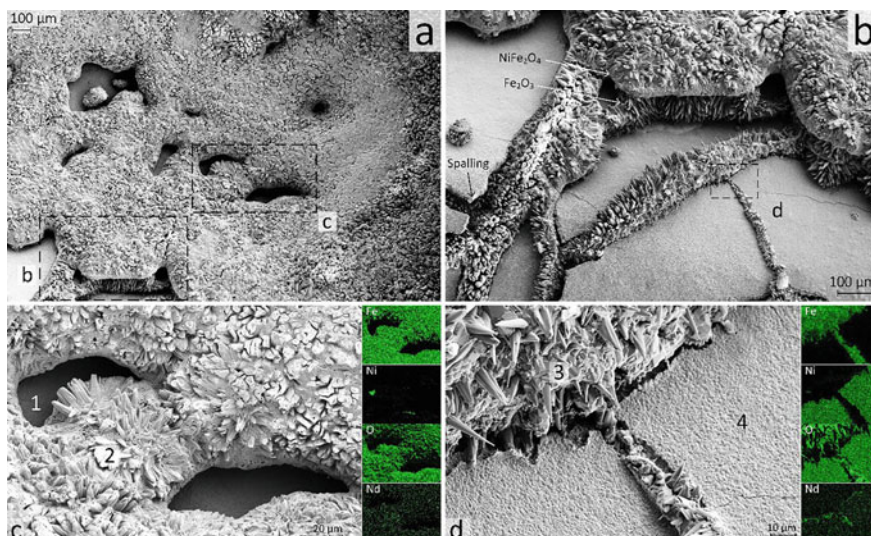

Fig. 9 SEM secondary electron images showing the surface of EOL NdFeB magnet sample oxidized at 1100 °C for 4 h. Also included are EDX element distribution maps for O, Fe, Ni, and Nd across the selected imaged area

in the current study is in line with these, where at 900 °C, the outer surface was, in general, homogenous with NiO but with some spiky Fe_2O_3 grown outward breaking the NiO layer. Furthermore, with longer oxidation time at 1100 °C, the NiO layer was diminished as it reacted with the Fe_2O_3 to form the spinel phase $NiFe_2O_4$ as its reaction is more thermodynamically favorable at higher temperatures.

Conclusion

The growth of oxides on the surface of the EOL NdFeB permanent magnet during the high-temperature oxidation at 900 and 1100 °C was investigated using in-situ hot-stage microscopy. Ex-situ scanning electron microscopy was utilized to supplement the analysis and to characterize the oxides. It was observed that at a lower temperature of 900 °C, the surface was covered by a NiO layer with some growth of a spiky Fe_2O_3 from inside which penetrated the NiO layer. This observation indicated that at 900 °C, the reaction between NiO and Fe_2O_3 was minimal. After four hours of oxidation, the NiO layer remained while the Fe_2O_3 continued to grow outward. At a higher temperature of 1100 °C, the Fe_2O_3 also grew from inside but at this temperature it immediately reacted with the NiO layer resulting in the formation of a $NiFe_2O_4$ layer. A longer period of oxidation at this temperature led to the $NiFe_2O_4$ entirely covering the surface. Both NiO at 900 °C and $NiFe_2O_4$ at 1100 °C, once covered the surface, appeared to significantly reduce further oxidation.

Conflict of Interest   The authors declare that they have no conflict of interest.

References

1. Chau K, Chan CC, Liu C (2008) Overview of permanent-magnet brushless drives for electric and hybrid electric vehicles. IEEE Trans Industr Electron 55(6):2246–2257
2. Lacal-Arántegui R (2015) Materials use in electricity generators in wind turbines—state-of-the-art and future specifications. J Clean Prod 87:275–283
3. München DD, Veit HM (2017) Neodymium as the main feature of permanent magnets from hard disk drives (HDDs). Waste Manag 61:372–376
4. Yang Y, Walton A, Sheridan R, Güth K, Gauß R, Gutfleisch O, Buchert M, Steenari B-M, Van Gerven T, Jones PT, Binnemans K (2017) REE recovery from end-of-life NdFeB permanent magnet scrap: a critical review. J Sustain Metall 3(1):122–149

5. Nababan DC, Mukhlis R, Durandet Y, Pownceby MI, Prentice L, Rhamdhani MA (2021) Mechanism and microstructure evolution of high temperature oxidation of end-of-life NdFeB rare earth permanent magnets. Corros Sci 182:109290

6. Zhang Y, Gu F, Su Z, Liu S, Anderson C, Jiang T (2020) Hydrometallurgical recovery of rare earth elements from NdFeB permanent magnet scrap: a review. Metals 10(6):841

7. Elwert T, Goldmann D, Roemer F, Schwarz S (2017) Recycling of NdFeB magnets from electric drive motors of (hybrid) electric vehicles. J Sustain Metall 3(1):108–121

8. Bailey G (2016) Life cycle assessment of the pyrometallurgical and hydrometallurgical recycling routes used in rare earth recycling: a case study of NdFeB magnets, Recycling 2016 Berlin, World Congress and Expo on Recycling, Date: 2016/07/25–2016/07/27. Berlin, Germany

9. Firdaus M, Rhamdhani MA, Rankin WJ, Pownceby M, Webster NAS, D'Angelo AM, McGregor K (2018) High temperature oxidation of rare earth permanent magnets. Part 1—microstructure evolution and general mechanism. Corros Sci 133:374–385

10. Firdaus M, Rhamdhani MA, Durandet Y, Rankin WJ, McGregor K (2018) High temperature oxidation of rare earth permanent magnets. Part 2–Kinetics. Corros Sci 133:318–326

11. Firdaus M, Rhamdhani MA (2018) High temperature recovery of rare earth ortho-ferrites from permanent magnets. In: Davis BR, Moats MS, Wang S, Gregurek D, Kapusta J, Battle TP, Schlesinger ME, Alvear Flores GR, Jak E, Goodall G, Free ML, Asselin E, Chagnes A, Dreisinger D, Jeffrey M, Lee J, Miller G, Petersen J, Ciminelli VST, Xu Q, Molnar R, Adams J, Liu W, Verbaan N, Goode J, London IM, Azimi G, Forstner A, Kappes R, Bhambhani T (eds) Extraction 2018. Springer International Publishing, Cham, pp 805–813

12. Firdaus M, Akbar Rhamdhani M, Durandet Y, John Rankin W, McGregor K, Webster NAS (2017) Microstructure observation of oxidation of Nd-magnet at high temperatures. In: Kim H, Alam S, Neelameggham NR, Oosterhof H, Ouchi T, Guan X (eds) Rare metal technology 2017. Springer International Publishing, Cham, pp 65–74

13. Nababan DC, Mukhlis R, Durandet Y, Pownceby MI, Prentice L, Rhamdhani MA (2021) Kinetics of high temperature oxidation of end-of-life Ni/Cu/Ni coated NdFeB rare earth permanent magnets. Corros Sci 189:109560